iScience

CellPress
OPEN ACCESS

Article

Oxytocin excites dorsal raphe serotonin neurons and bidirectionally gates their glutamate synapses

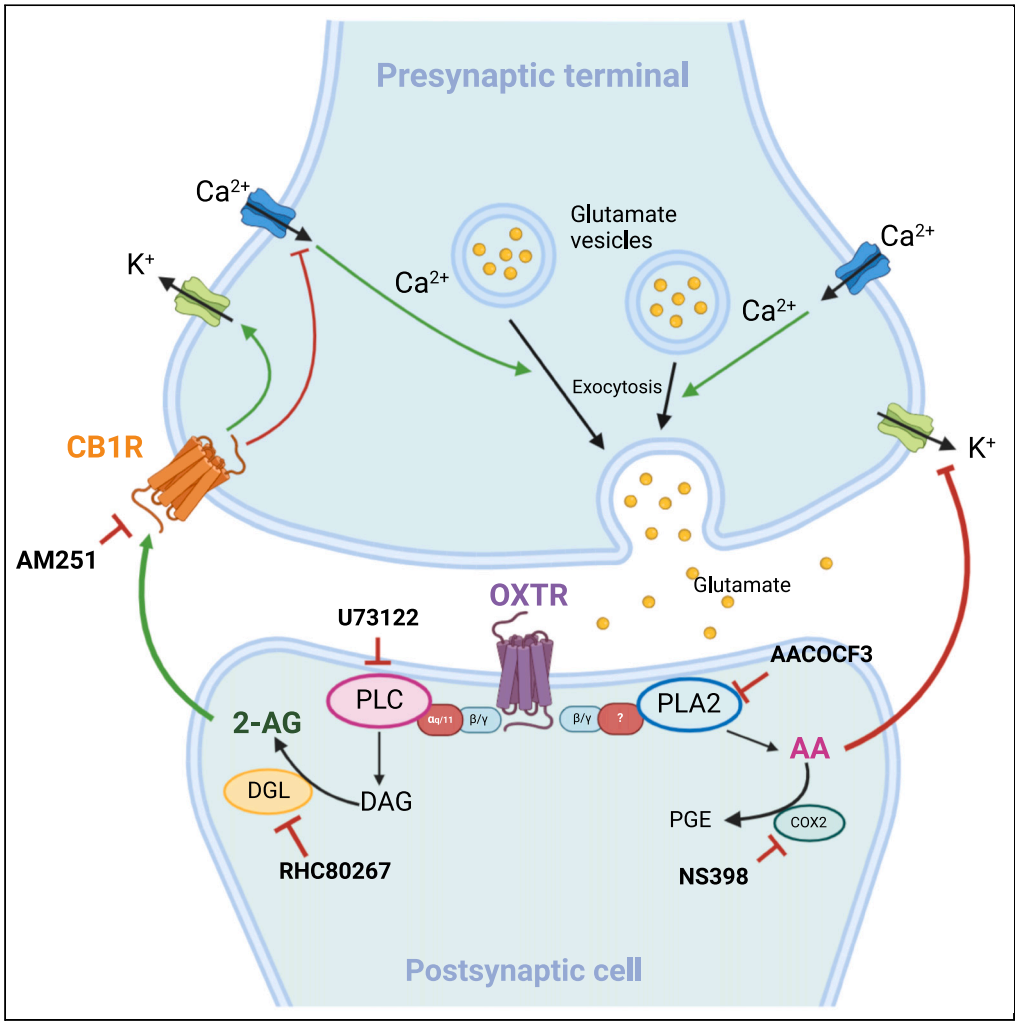

Saida Oubraim, Roh-Yu Shen, Samir Haj-Dahmane

sh38@buffalo.edu

Highlights

OXT excites and alters the firing activity of DRN 5-HT neurons

OXT induces target-specific depression and potentiation of DRN glutamates synapses

Retrograde 2-AG signaling mediates OXT-induced synaptic depression

Retrograde AA signaling mediates OXT-induced synaptic potentiation

Oubraim et al., iScience 26, 106707
May 19, 2023
https://doi.org/10.1016/j.isci.2023.106707

iScience

CellPress
OPEN ACCESS

Article

Oxytocin excites dorsal raphe serotonin neurons and bidirectionally gates their glutamate synapses

Saida Oubraim,[1] Roh-Yu Shen,[1,2] and Samir Haj-Dahmane[1,2,3,*]

SUMMARY

Oxytocin (OXT) modulates wide spectrum of social and emotional behaviors via modulation of numerous neurotransmitter systems, including serotonin (5-HT). However, how OXT controls the function of dorsal raphe nucleus (DRN) 5-HT neurons remains unknown. Here, we reveal that OXT excites and alters the firing pattern of 5-HT neurons via activation of postsynaptic OXT receptors (OXTRs). In addition, OXT induces cell-type-specific depression and potentiation of DRN glutamate synapses by two retrograde lipid messengers, 2-arachidonoylglycerol (2-AG) and arachidonic acid (AA), respectively. Neuronal mapping demonstrates that OXT preferentially potentiates glutamate synapses of 5-HT neurons projecting to medial prefrontal cortex (mPFC) and depresses glutamatergic inputs to 5-HT neurons projecting to lateral habenula (LHb) and central amygdala (CeA). Thus, by engaging distinct retrograde lipid messengers, OXT exerts a target-specific gating of glutamate synapses on the DRN. As such, our data uncovers the neuronal mechanisms by which OXT modulates the function of DRN 5-HT neurons.

INTRODUCTION

The nonapeptide oxytocin (OXT) is an evolutionarily conserved hormone well known for its role in parturition and the onset of lactation.[1,2] In mammalian brain, OXT is mainly synthesized in magnocellular neurons of the hypothalamus, located in the supraoptic (SON), paraventricular (PVN),[3,4] and accessory nuclei.[5,6] In addition to neurohypophysis afferences, oxytocinergic neurons project extensively to the forebrain, including medial prefrontal cortex (mPFC),[7] septum,[8] central amygdala (CeA),[9] parts of the brainstem area[6] and dorsal raphe nucleus (DRN).[10] The physiological effects of OXT are largely mediated by a single OXT receptor (OXTR) belonging to $G_{q/11}$ G-protein-coupled receptor (GPCR) family[11] and highly expressed throughout the brain.[12,13] Consequently, by controlling the activity of complex neuronal networks, OXTRs regulate wide spectrum of behaviors including social,[14,15] maternal behaviors,[16] anxiety-related behaviors,[17] food intake,[18] stress responses,[17,19] and pain.[20]

OXT interacts with others neurotransmitters, including serotonin (5-HT) to modulate an array of socio-affective behaviors. Indeed, the DRN, a major source of 5-HT to the forebrain, receives oxytocinergic fibers[10] and expresses OXTRs.[21,22] In rodent, activation of these receptors increases 5-HT release, reduces anxiety-related behaviors,[22] enhances social reward,[23] and decreases aggression behaviors.[24,25] Oxytocinergic signaling in the DRN also regulates the normal development and expression of maternal social and affective behaviors.[21,26] For instance, postpartum genetic deletion of DRN OXTRs increases pups loss after parturition, impairs nursing, increases aggression, and behavioral despair.[21] In addition, numerous studies have reported that 5-HT regulates the function of PVN oxytocinergic neurons.[27,28] This functional cross-talk between OXT and 5-HT systems is involved in several neurodevelopmental disorders, including autism spectrum disorders (ASD).[14,29,30] Thus, animal and human studies have revealed an altered function of OXT and 5-HT systems in ASD.[29,31,32] Importantly, pharmacological manipulations of OXT signaling improves social and emotional deficits associated with ASD, at least in part, by recruiting the 5-HT system.[23,33–35]

Although the role of OXT-5-HT interaction in controlling socio-affective behaviors is well established, the precise mechanisms by which OXT controls the function of 5-HT neurons and synaptic dynamic in DRN remain unknown. Here, we show that activation of OXTRs excites DRN 5-HT neurons, alters their firing pattern, and

[1]Department of Pharmacology and Toxicology, University at Buffalo, Jacobs School of Medicine and Biomedical Sciences, State University of New York, 1021 Main Street, Buffalo, NY 14203, USA

[2]University at Buffalo Neuroscience Program, University at Buffalo, Jacobs School of Medicine and Biomedical Sciences, State University of New York, 1021 Main Street, Buffalo, NY 14203, USA

[3]Lead contact

*Correspondence: sh38@buffalo.edu

https://doi.org/10.1016/j.isci.2023.106707

induces target-specific depression and potentiation of glutamate synapses. This bidirectional gating is signaled by two distinct retrograde lipid messengers, the endocannabinoid 2-arachidonoylglycerol (2-AG) and arachidonic acid (AA), respectively. As such, the present study unravels novel cellular mechanisms by which OXT modulates the function of DRN 5-HT neurons.

RESULTS

All electrophysiological recordings were performed from neurons located in dorsal-medial (dmDRN) and ventral-medial (vmDRN) regions of the DRN. Serotonin neurons were identified using three criteria: (1) they display a resting membrane potential around −60 mV, (2) low-frequency and regular firing action potentials (1–2 Hz) following injection of suprathreshold depolarizing current pulses, and (3) a pronounced aflterhyperpolarizing potential (AHP).[36,37] Using a post-hoc tryptophan hydroxylase type 2 (Tph2) immunohistochemical labeling, we and others have previously shown that all DRN neurons that exhibit these properties were Tph2 positive neurons.[38]

Oxytocin excites and alters the firing pattern of putative DRN 5-HT neurons

To assess the effects of OXT on the excitability of DRN 5-HT neurons, we first used cell-attached recordings and examined the effects of bath application of OXT on their spontaneous firing activity. As reported previously,[36,37] most sampled DRN 5-HT neurons were either quiescent or exhibit very low regular spontaneous firing (Control: 0.26 ± 0.04 Hz, n = 10, Figure 1A$_1$). Administration of OXT (1 μM) increased the spontaneous firing activity in 77% of sampled DRN neurons (OXT: 0.54 ± 0.08 Hz, n = 10, p = 0.0064 vs. control, Figures 1A and 1B). In the remaining 23% of neurons, OXT shifted their firing pattern from slow regular to high burst firing (n = 4, Figure 1C). Next, using whole-cell recordings, we assessed the effect of OXT on the resting membrane potential and found that OXT (1 μM) induced a strong membrane depolarization that triggered action potential firing (n = 8, Figure 1D). In DRN 5-HT neurons clamped at −65 mV, and in the presence of voltage-dependent sodium channel blocker tetrodotoxin (TTX, 1 μM), OXT caused a significant inward shift of the holding current (I_{OXT}), which was blocked by OXTR antagonist (d(CH$_2$)$_5^1$,Tyr(-Me)^2,Orn^8)-Oxytocin trifluoroacetate salt (OTA,10 μM) (OXT_{CTRL}: 24.23 ± 5.46 pA; OXT_{OTA}: 3.22 ± 2.84 pA, n = 6; p = 1.20E-4, Figure 1E). The inward current was also induced by a selective OXTR agonist (Thr^4,Gly^7)-Oxytocin (TGO,1 μM) and was blocked with OTA (1 μM) (TGO_{CTRL}: 27.63 ± 3.73 pA, TGO_{OTA}: 3.36 ± 2.90, n = 6; p = 3.90E-6, Figure 1F). Importantly, The OXT-induced inward current (I_{oxt}) was abolished by inhibition of postsynaptic G-protein signaling with guanosine-5′-(β-thio)-diphosphate (GDPβS) (I_{OXT} GTP: 24.85 ± 4.53 pA, I_{oxt} GDP$_\beta$S: 3.96 ± 1.62 pA, n = 7; p = 0.0033; Figure 1G), indicating that it was signaled by activation of G-protein. Collectively, these results demonstrate that OXT depolarizes and increases the excitability of putative DRN 5-HT neurons via activation of postsynaptic OXTRs.

Oxytocin bidirectionally gates the strength of DRN glutamate synapses

We also interrogated the effects of OXT on the strength of glutamatergic inputs to putative DRN 5-HT neurons, by examining the impact of OXT on the amplitude of evoked excitatory postsynaptic currents (eEPSCs). We found that in a group of neurons (n = 18), OXT (1 μM) significantly depressed the amplitude of eEPSCs. This effect was blocked by OXTR antagonist OTA (10 μM) (OXT_{CTRL}: 70.82 ± 1.97% of baseline, n = 18; OXT_{OTA}: 101.93 ± 3.39% of baseline, n = 12; p = 1.99E-15; Figure 2A). Similar results were obtained using the selective OXTR agonist TGO (1 μM) (TGO_{CTRL}: 68.74 ± 8.01%, n = 8; TGO_{OTA}: 97.57 ± 4.99%, n = 5; p = 0.007; Figure 2B), thereby indicating that OXTRs signal the inhibition of eEPSCs. Examination of the paired pulse ratio (PPR) and coefficient of variance (CV) of eEPSCs, two independent measures of the probability of glutamate release, showed that the depression of eEPSCs was consistently accompanied by a significant increase in both PPR (Control: 1.11 ± 0.09; OXT: 1.29 ± 0.13, n = 6, p = 0.013, Figure 2C) and CV (Control: 0.31 ± 0.04, OXT: 0.42 ± 0.05, n = 6, p = 0.0046 control vs. OXT, Figure 2D), indicating that OXTRs depress glutamate DRN synapses by inhibiting glutamate release.

In another group of 5-HT neurons, OXT (1 μM) was found to potentiate the amplitude of eEPSCs. This effect was also readily blocked by OTA (10 μM), a selective OXTR antagonist (OXT_{CTRL}: 152.71 ± 11.19% of baseline, n = 8, OXT_{OTA}: 103.95 ± 3.63% of baseline, n = 15; p = 6.18E-8; Figure 2E) and mimicked by selective OXTR agonist TGO (1 μM) (TGO_{CTRL}: 144.81 ± 8.29%, n = 11; TGO_{OTA}: 105.92 ± 6.89%, n = 7; p = 3.36E-4; Figure 2F). The OXTR-induced potentiation of eEPSCs was accompanied by a decrease in PPR (Control: 1.47 ± 0.15; OXT: 1.21 ± 0.11, n = 6, p = 0.025, vs. control, Figure 2G) and CV (control: 0.45 ± 0.04;

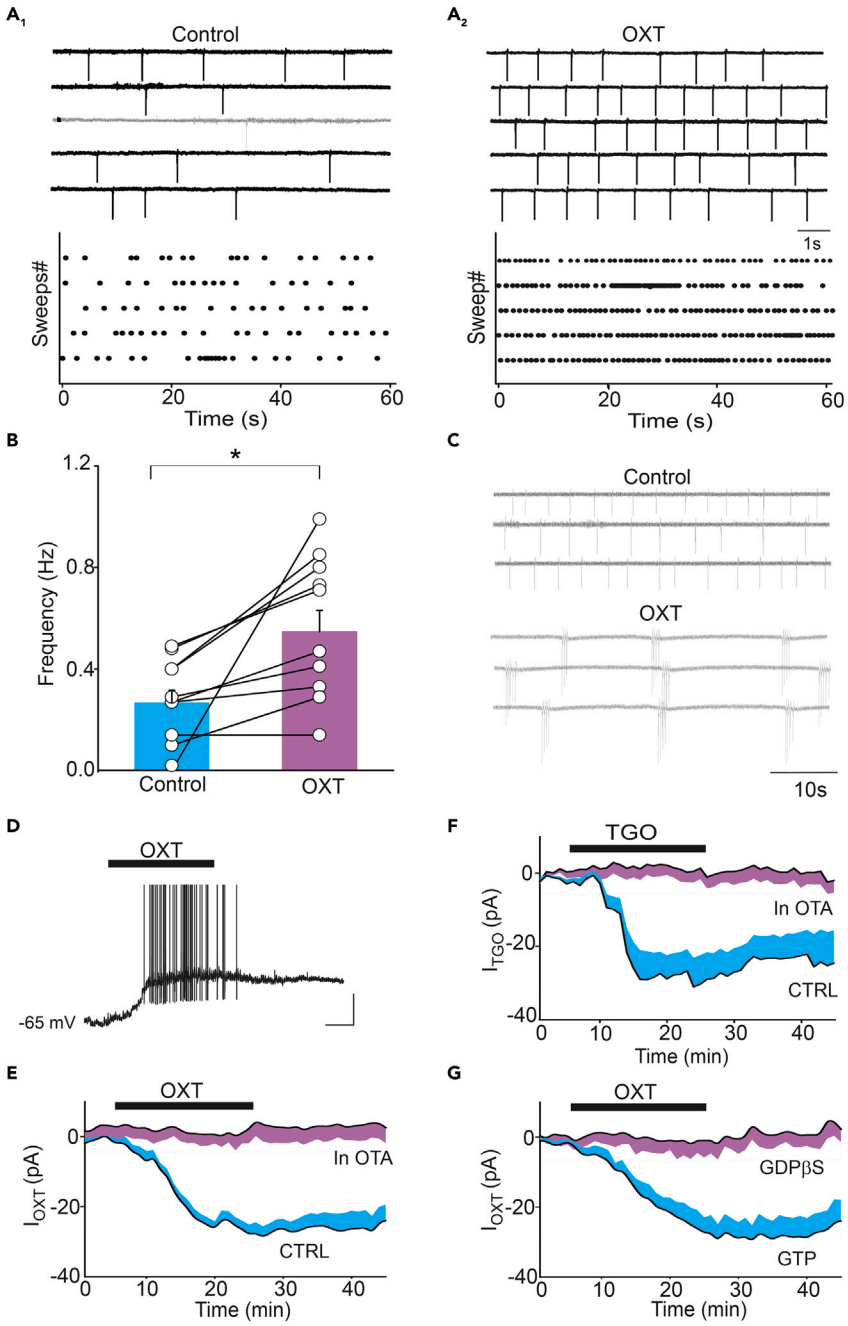

Figure 1. Oxytocin increases the excitability of DRN 5-HT neurons

(A_1-A_2) Representative traces of cell-attached recordings (top panels) and scatterplots of spontaneous firing of Putative DRN 5-HT neurons (lower panels) recorded in control (A_1) and during bath application of OXT (1 μM) (A_2).

(B) Average spontaneous firing frequency recorded in control and in the presence of OXT (n = 10, p = 0.0064).

(C) Voltage traces of cell-attached recording from Putative DRN 5-HT neurons obtained in control (Upper traces) and in OXT (lower traces). Note that OXT switched the firing form regular to burst spiking.

(D) Current clamp recording of the membrane depolarization from a DRN 5-HT neuron induced by OXT (1 μM).

(E) Average amplitude and time course of inward currents (I_{oxt}) induced by OXT (1 μM) in control and in the presence of OXTR antagonist OTA (1 μM, p = 0.027) recorded from Putative DRN 5-HT neurons voltage clamped at −70 mV.

(F) Average amplitude and time course of inward currents induced by TGO (1 μM) in control and in the presence of OTA (1 μM) recorded from DRN 5-HT neurons at −70 mV.

(G) OXT-induced inward current (I_{oxt}) recorded with GTP and GDPβS.

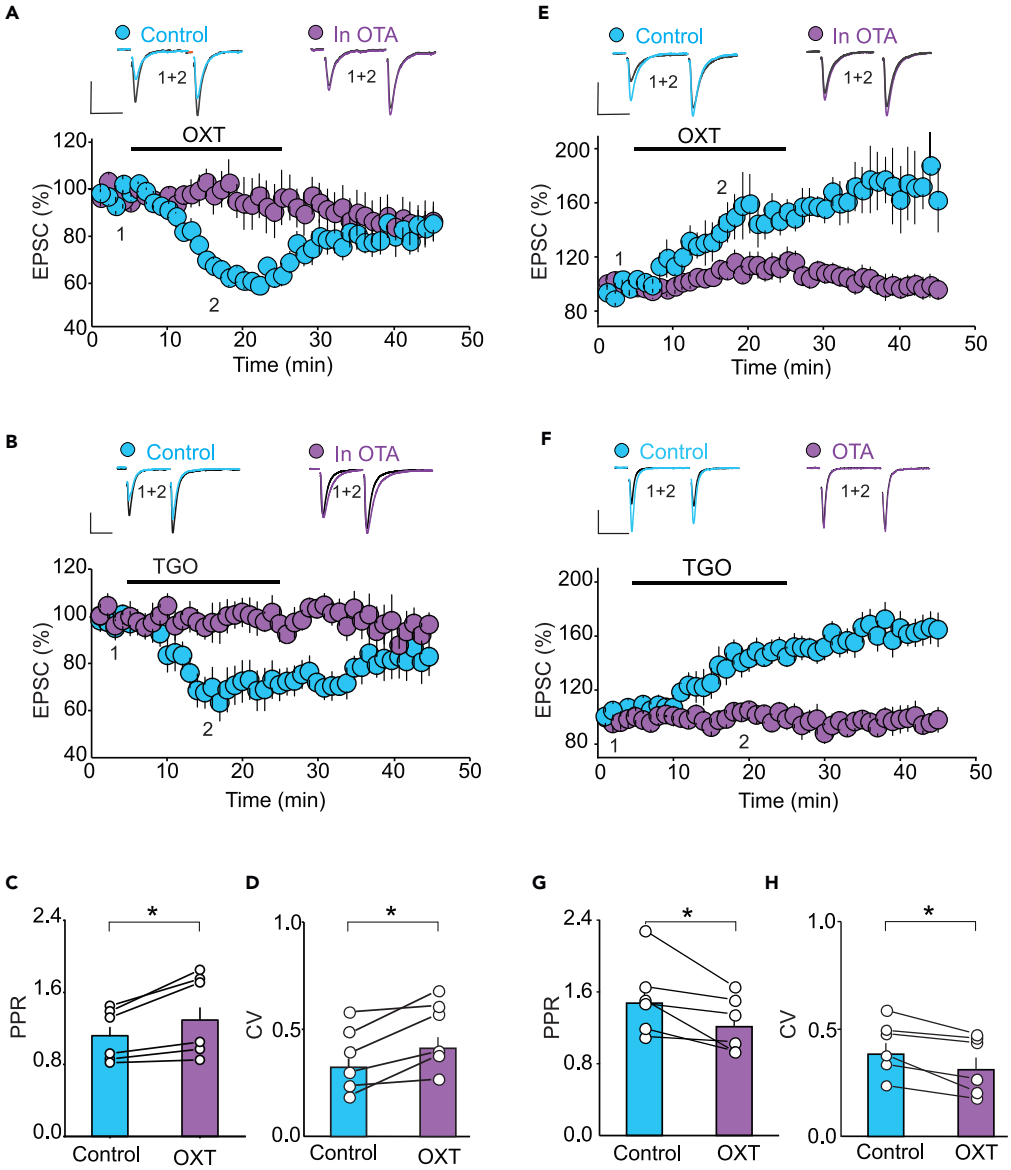

Figure 2. OXT receptors bidirectionally regulate the strength of glutamate synapses to DRN 5-HT neurons

(A) Lower graph, depression of eEPSCs induced by OXT (1 μM) in control (●, n = 18, p = 7.87E-11) and in OTA (1 μM, ●, n = 12, p = 0.26) Upper panel, eEPSC traces taken as indicated in lower panel. Scale bars: 50 pA, 50 ms.

(B) Lower graph, depression of eEPSCs induced by TGO (1 μM) in control (●, n = 8, p = 0.0064) and in OTA (1 μM) (●, n = 5, p = 0.65). Upper graph, eEPSC traces taken as indicated in lower panel.

(C) PPR of eEPSCs before and during OXT-induced depression (n = 6, p = 0.013).

(D) CV of eEPSCs before and during OXT-induced inhibition (n = 6, p = 0.0046).

(E) Potentiation of eEPSCs induced by OXT (1 μM) in control (●, n = 8, p = 0.0013) and in OTA (1 μM, ●, n = 15, p = 0.13). Upper graph, eEPSC traces collected as indicated in lower graph.

(F) Lower panel, potentiation of eEPSCs induced by TGO (1 μM) in control (●, n = 11, p = 2.46E-4) and in OTA (●, n = 7, p = 0.42). Upper panel, eEPSC traces taken as indicated in lower graph.

(G) PPR of eEPSCs in control and in OXT (n = 6, p = 0.025).

(H) CV of eEPSCs in control and in OXT (n = 6, p = 0.037). Scale bars: 50 pA, 25 ms.

OXT: 0.32 ± 0.06, n = 6, p = 0.037 vs. control, Figure 2H), indicating an increase in glutamate release. Collectively, these results indicate that OXT bidirectionally regulates the strength of glutamate synapses in different subpopulations of putative DRN 5-HT neurons.

Oxytocin depresses DRN glutamate synapses via retrograde endocannabinoid signaling

To determine the mechanisms of OXT-induced depression of glutamate release, we first examined whether this effect was signaled by pre or postsynaptic OXTRs. To that end, we assessed the impact of inhibiting postsynaptic G-protein signaling with intracellular application of $GDP_{\beta}S$ on OXTR-induced inhibition of eEPSC amplitude. We found that postsynaptic intracellular application of $GDP_{\beta}S$, which inhibited OXTRs as indicated by the blockade of I_{OXT} (Figure 1F), also abolished the inhibition of eEPSCs (OXT_{GTP}: 68.10 ± 1.18% of baseline, n = 10; $OXT_{GDP\beta S}$: 98.88 ± 5.84% of baseline, n = 13; p = 2.54E-8; Figure 3A). This finding indicates that the OXT-induced depression of glutamate synapses is mediated by postsynaptic OXTRs and involves retrograde messengers. Next, because OXTRs are coupled to $G_{q/11}$ type G-protein, activation of which induces endocannabinoid (eCB) synthesis and release,[39,40] we examined whether the depression of glutamate release is signaled by retrograde eCB signaling. Blocking CB1Rs with AM 251 (3 μM) abolished the OXT-induced depression of eEPSC amplitude (OXT_{CTRL}: 68.91 ± 1.24% of baseline, n = 10, $OXT_{AM\ 251}$: 95.48 ± 3.20% of baseline, n = 12; p = 7.67E-12; Figure 3B). Collectively, these results indicate that activation of postsynaptic OXTRs depresses DRN glutamate synapses via retrograde eCBs.

OXT receptors activate phospholipase C (PLC) leading to the formation of 1, 2 diacylglycerol (1,2 DAG),[41,42] which in turn is cleaved by diacylglycerol lipase (DAGL) to produce the eCB 2-arachidonoylglycerol (2-AG).[43,44] To test whether retrograde 2-AG mediates the depression of glutamate synapses, we examined the effect of PLC inhibitor U73122 on the OXTR-induced depression of eEPSCs. Treatment of DRN slices with U73122 (10 μM) but not its inactive analog U73433 (10 μM), blocked the OXTR-induced depression of eEPSC amplitude (OXT_{U73122}: 111 ± 8.08% of baseline, n = 10, p = 0.20 vs. baseline; OXT_{U73343}: 56.55 ± 2.95% of baseline, n = 9, p = 3.56E-7 vs. baseline; Figure 3C). Similar to the effect of PLC inhibitor, treatment of DRN slices with the DAGL inhibitor RHC80267 (50 μM) prevented the OXTR-induced inhibition of eEPSC amplitude (OXT_{CTRL}: 60.32 ± 2.03% of baseline, n = 7; $OXT_{RHC80267}$: 106.29 ± 7.25% of baseline, n = 12; p = 1.38E-6; Figure 3D). Collectively, these results indicate that activation of PLC/DAGL signaling cascade and the release of retrograde 2-AG mediates the OXTRs-induced depression of glutamate synapses of DRN 5-HT neurons.

Oxytocin potentiates DRN glutamate synapses via retrograde arachidonic acid

To determine the mechanisms of OXT-mediated potentiation of glutamate synapses of putative DRN 5-HT neurons, we first assessed the role of postsynaptic OXTRs, by examining the effects of postsynaptic G-protein inhibition on OXT-induced potentiation of eEPSCs. Consistent with an effect mediated by postsynaptic OXTRs, our results revealed that intracellular application of $GDP_{\beta}S$, which blocked I_{OXT} (see Figure 1F), also abolished the potentiation of DRN glutamate synapses (OXT_{GTP}: 156.48 ± 12.17% of baseline, n = 7; $OXT_{GDP\beta S}$: 98.84 ± 4.39%, n = 13; p = 8.24E-8; Figures $4A_1$-A_2). Because OXTRs are coupled to PLC signaling pathways,[45] we next tested the involvement of this signaling cascade and found that inhibition of PLC with U73122 (5 μM), had no effect on OXT-induced potentiation of eEPSC amplitude (OXT_{U73343}: 146.81 ± 11.99% of baseline, n = 7; OXT_{U73122}: 157.26 ± 12.5% of baseline, n = 12; p > 0.5; Figures $4B_1$-B_2). Similarly, inhibition of DAGL with RHC80267 (50 μM), did not affect the magnitude of OXT-induced potentiation of eEPSCs (OXT_{CTRL}: 146.85 ± 7.01% of baseline, n = 5; $OXT_{RHC80267}$: 157.56 ± 13.26% of baseline, n = 6; p > 0.5; Figures $4C_1$-C_2). Collectively, these results indicate that while mediated by postsynaptic OXTRs, the OXT-induced potentiation of eEPSCs in putative DRN 5-HT neurons is not signaled by PLC/DAGL downstream cascade.

Stimulation of OXTRs also activates cytosolic phospholipase A2 ($cPLA_2$) and enhances the release of arachidonic acid (AA),[46,47] raising the possibility that $cPLA_2$/AA signaling cascade could mediate the OXTR-induced potentiation of glutamate synapses. This possibility was tested by assessing the impact of inhibiting $cPLA_2$ with AACOCF3 on the OXT-induced potentiation of EPSC amplitude. Results of this experiments showed that the $cPLA_2$ inhibitor AACOCF3 (20 μM) abolished OXTR-induced potentiation of eEPSC amplitude (OXT_{CTRL}: 141.36 ± 6.80% of baseline, n = 6, $OXT_{AACOCF3}$: 102.95 ± 4.03% of baseline, n = 12; p = 3.62E-5; Figure 5A). In contrast, direct administration of AA (10 μM) mimicked the effect of OXT and induced potentiation of eEPSC amplitude (AA: 159.96 ± 8.15% of baseline, n = 9, p = 3.23E-6 vs. baseline; Figure 5B) similar to that obtained with OXT (OXT: 144.15 ± 6.97% of baseline, n = 6, p = 0.0018 vs. baseline; Figure 5B). Taken together, these results indicate that activation of $cPLA_2$ and the increase in AA signaling mediate the OXTR-induced potentiation of glutamate synapses to DRN 5-HT neurons.

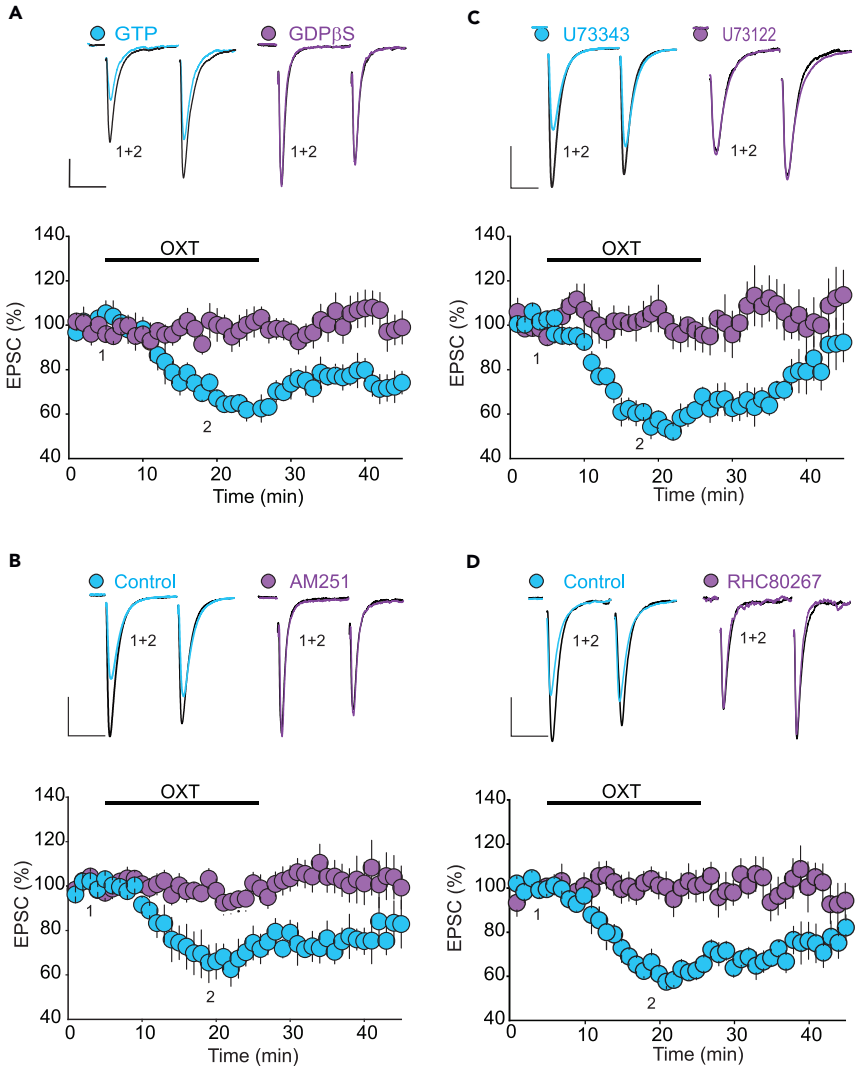

Figure 3. Oxytocin inhibits DRN glutamate synapses via retrograde 2-AG signaling

(A) Blockade of postsynaptic G-protein signaling with GDPβS abolishes the OXT-induced depression of eEPSC amplitude. Lower panel is a summary of the depression of eEPSCs induced by OXT (1 μM) using an intracellular solution containing either GTP (●, n = 10 = 28.02, p) or GDPβS (●, n = 13, p = 0.97). Upper graphs are representative eEPSC traces taken at time points indicated by numbers in lower panel. Scale bars: 50 pA, 20 ms.

(B) Blocking CB1Rs abolishes the OXT-induced depression of eEPSC amplitude. Lower graph is a summary of the OXT-induced depression of eEPSCs obtained in control (●, n = 10, p = 1.27E-9) and in slices treated with the CB1R antagonist AM 251 (5 μM, ●, n = 12, p = 0.18). Upper graphs are sample eEPSC traces collected at the time points noted in the lower panel. Scale bars: 50 pA, 20 ms.

(C) Inhibition of PLC prevents the OXT-induced depression of eEPSCs. Lower graph summarizes the OXT-induced inhibition of eEPSCs obtained in slices treated with the PLC inhibitor U73122 (5 μM, ●, n = 10, p = 0.20) or its inactive analog U73343 (5 μM, ●, n = 9, p = 3.56E-7). Upper graphs are representative eEPSC traces collected at the time points indicated by numbers in lower graph. Scale bars: 50 pA, 25 ms.

(D) Inhibition of diacylglycerol lipase (DAGL) prevents the OXT-induced depression of eEPSCs. Lower panel is a summary of the inhibition of eEPSC amplitude induced by OXT (1 μM) obtained in control (●, n = 7, p = 1.34E-6) and in slices treated with the DAGL inhibitors RHC80267 (50 μM, ●, n = 12, p = 0.33). Upper graphs are representative eEPSC traces taken at time points indicated in lower graph. Scale bars: 25 pA, 25 ms.

Arachidonic acid is readily metabolized onto prostaglandins (PGs) by cyclooxygenase type 2 (COX2), an enzyme highly expressed in DRN neurons.[48] These AA metabolites modulate synaptic strength in other brain areas via PG receptors,[49] which are expressed in the DRN.[50] Thus, we sought to determine the

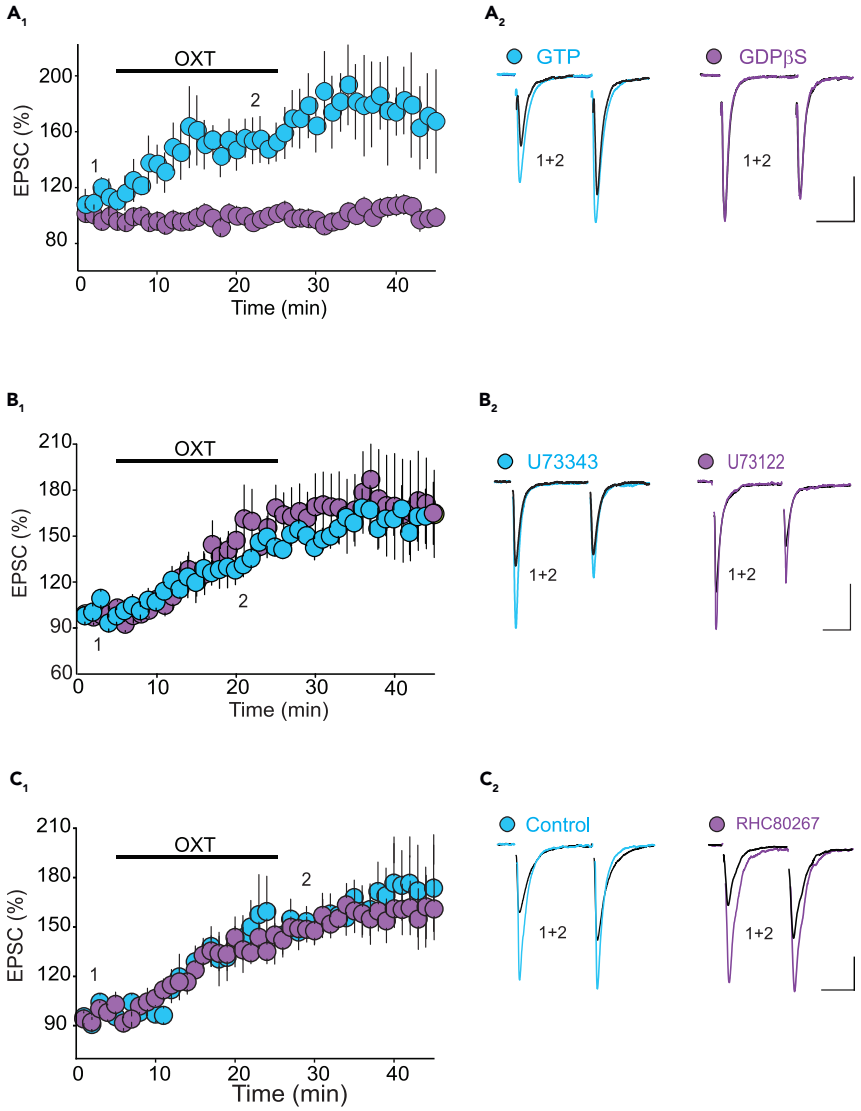

Figure 4. The potentiation of DRN glutamate synapses is not mediated by PLC/DAGL signaling cascade

(A_1-A_2) Inhibition of postsynaptic G-protein signaling abolishes OXT-induced potentiation of DRN glutamate synapses. (A_1) Summary of OXT-induced potentiation of eEPSC amplitude recorded with an internal solution containing GTP (●, n = 7, p = 0.0035) or GDPβS (●, n = 13, p = 0.97). (A_2) eEPSC traces collected at time points indicated in the left panel. (B_1-B_2) Inhibition of PLC signaling does not alter OXT-induced potentiation of eEPSCs. (B_1) Summary of OXT-induced increase in eEPSC amplitude recorded in slices treated with the PLC inhibitor U73122 (5 μM, ●, n = 7, p = 0.0055) or its inactive analog U73343 (5 μM, ●, n = 12, p = 7.94E-4). (B_2) eEPSC traces collected at time points indicated in panel B_1. (C_1-C_2) Inhibition of DAGL has no effect on OXT-induced potentiation of eEPSC amplitude. (C_1) Summary of OXT-induced increase in eEPSC amplitude obtained in control (●, n = 5, p = 8.44E-4) and in slices treated with DAGL inhibitor RHC80267 (50 μM, ●, n = 6, p = 0.0078). (C_2) Sample eEPSC traces collected at time points indicated in graph C_1. Scale bars: 50 pA, 25 ms.

involvement of AA/COX2 downstream products by assessing the impact of COX2 inhibitors on OXTR-induced potentiation of DRN glutamate synapses. The results showed that the COX2 inhibitor N-(2-cyclohexyloxy-4-nitrophenyl) methanesulfonamide (NS398, 40 μM) had no effect on OXT-induced potentiation of eEPSC amplitude (OXT_{CTRL}: 141.03 ± 6.90% of baseline, n = 6; OXT_{NS398}: 133.32 ± 6.25% of baseline, n = 6; p > 0.5; Figure 5C), thereby ruling out the involvement of COX2 downstream products. AA can also directly inhibit voltage-gated potassium channels (Kv),[51,52] including presynaptic A-type channels,[53–55] inhibition of which increases neurotransmitter release.[56] Therefore, to test whether AA

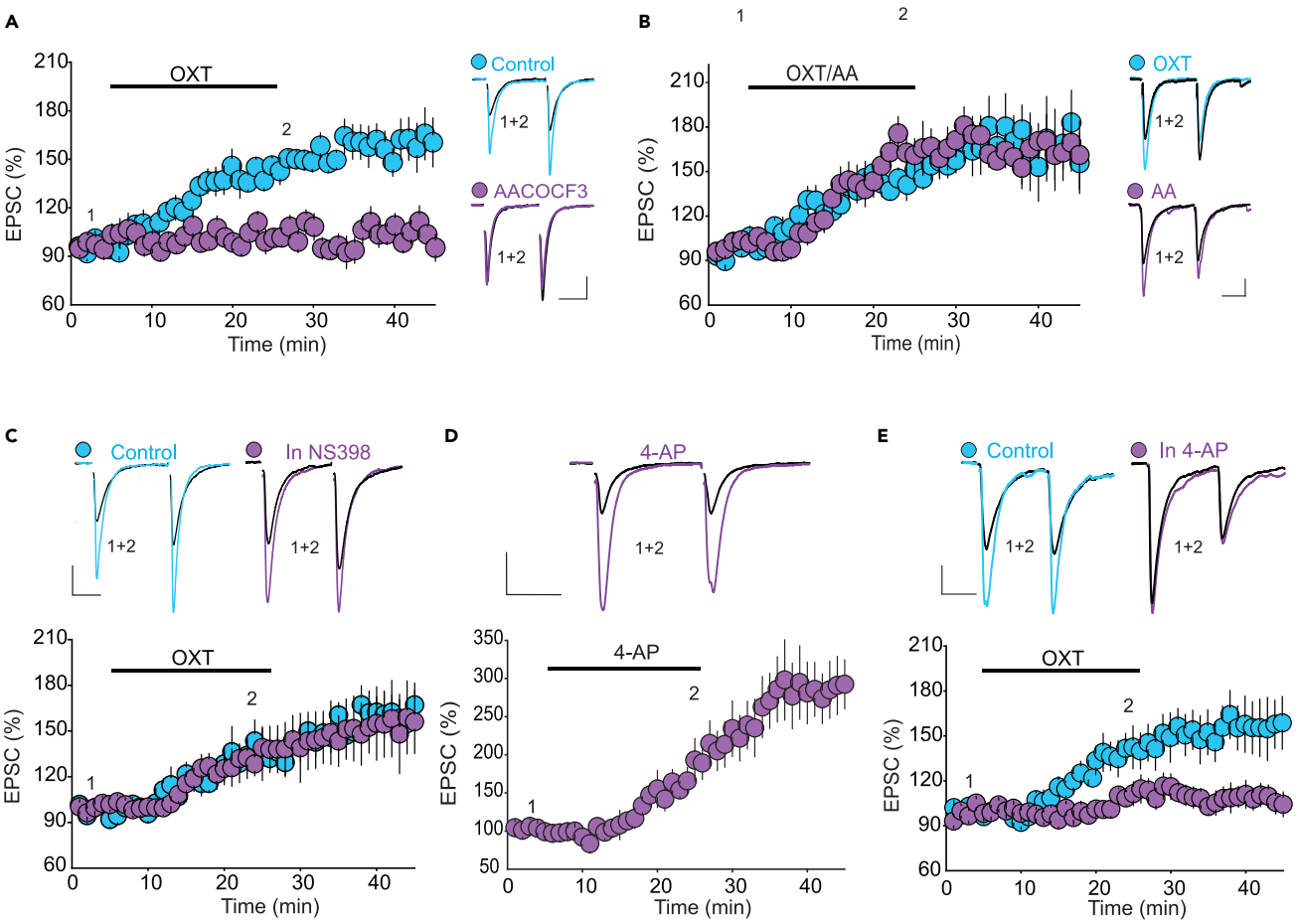

Figure 5. Oxytocin potentiates DRN glutamate synapses via PLA_2-arachidonic acid pathway

(A) Inhibition of PLA_2 blocks OXT-induced potentiation of eEPSC amplitude. Left graph, summary of OXT-induced potentiation of eEPSC amplitude obtained in control (●, n = 6, p = 6.87E-4) and in the presence of PLA_2 inhibitor AACOCF3 (20 μM, ●, n = 12, p = 0.26). Right panel, sample eEPSC traces recorded at time points indicated in left panel.

(B) Bath application of AA mimics OXT-induced potentiation of eEPSC amplitude. Left panel, summary of the enhanced eEPSC amplitude induced by OXT (●, n = 6, p = 4.29E-4) and AA (10 μM, ●, n = 9, p = 4.04E-4). Right panel, representative eEPSCs recorded at time points indicated in the left panel.

(C) Inhibition of COX2 inhibitor does not alter the effect of OXT on eEPSCs amplitude. Lower panel, summary graph of OXT-induced potentiation of eEPSC amplitude obtained in control (●, n = 6, p = 0.0014) and in slices treated with COX2 inhibitor NS398 (10 μM, ●, n = 6, p = 0.015). Upper graph, representative eEPSC traces recorded at time points indicated in lower graph.

(D) Blockade of voltage-dependent potassium channels mimics the OXT-induced potentiation of eEPSC amplitude. Lower panel, summary of the potentiation of eEPSC induced by 4-AP (50 μM). Upper graph, sample eEPSC traces at time points indicated in lower panel.

(E) Blockade of voltage-dependent potassium channels with 4-AP occludes OXT-induced potentiation of eEPSC amplitude. Lower graph, summary of OXT-induced increase in eEPSC amplitude recorded in control (●, n = 5, p = 0.019) and in slices treated with 4-AP (50 μM, ●, n = 7, p = 0.114). Upper graph, representative eEPSCs traces taken at time points indicated in lower panel. Scale bars for all graphs: 25 pA, 25 ms.

signals OXTR-induced potentiation of glutamate synapses by inhibiting A-type potassium, we examined whether blockade of these channels can mimic and occlude the effect of OXTRs. We found that bath application of 4-AP (50 μM), a blocker of A-type potassium channels, induced a robust potentiation of eEPSCs (4-AP: 270 ± 8.33%, n = 5, p = 0.010 vs. baseline, Figure 5D) and decreased the PPR (PPR baseline: 0.98 ± 0.06, PPR 4-AP: 0.69 ± 0.03, n = 5, p = 0.01 vs. baseline). Importantly, pretreatment of DRN slice with 4-AP occluded and prevented the OXTR-induced potentiation of glutamate synapses (OXT_{CTRL}: 145.14 ± 10.23% of baseline, n = 6; $OXT_{4\text{-}AP}$: 113.39 ± 7.59% of baseline, n = 7; p = 0.036; Figure 5E), suggesting that inhibition of K^+ channels mediates the effects of OXT. Collectively, these results suggest that the OXT-induced potentiation of glutamate synapses in a subpopulation of putative DRN 5-HT neurons is mediated by activation of $cPLA_2$ and generation of AA, which inhibits K^+ channels and enhances glutamate release.

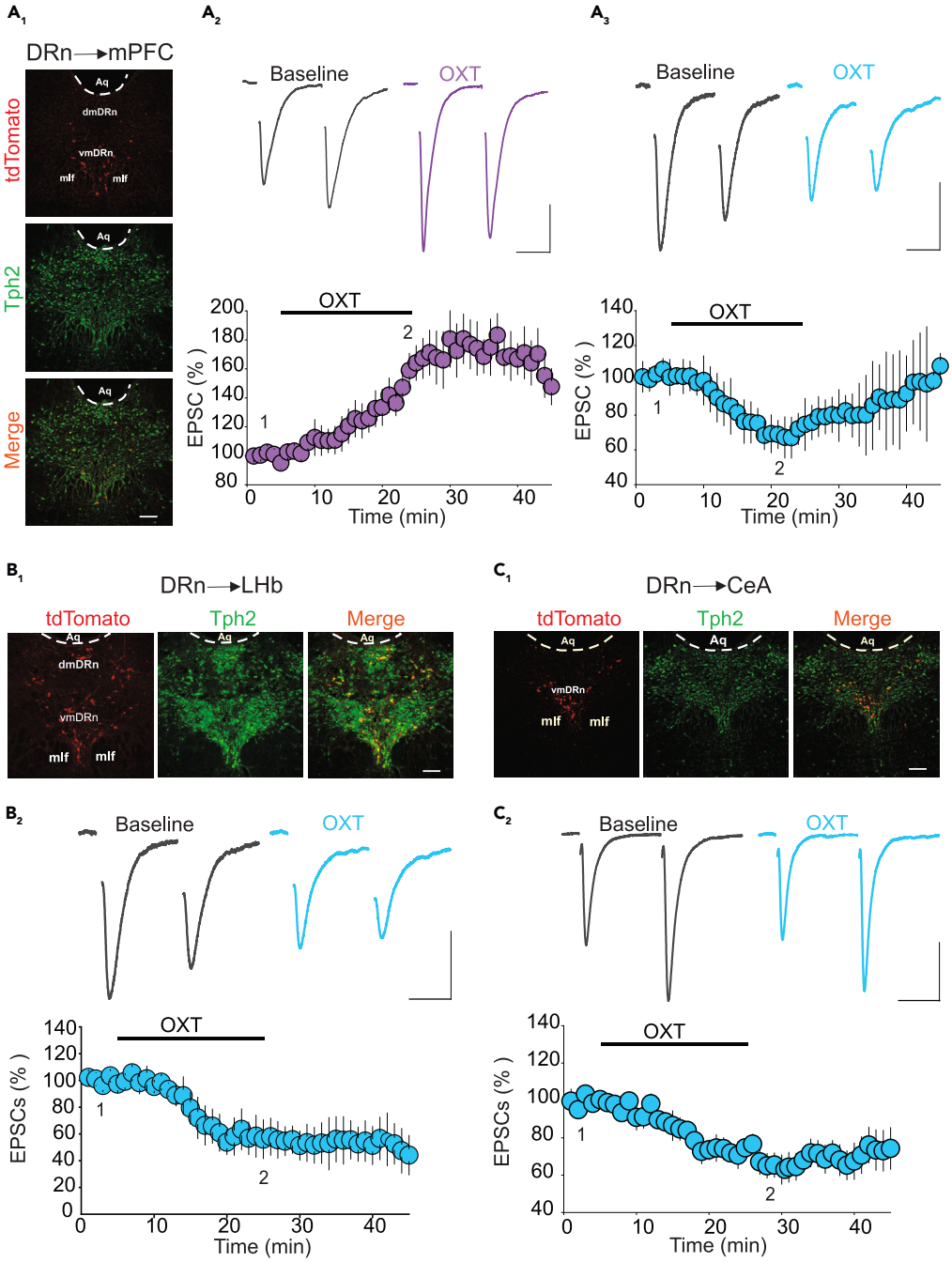

Figure 6. Oxytocin induces Cell-type-specific gating of DRN glutamate synapses

(A_1) Fluorescence images of DRN coronal sections showing mPFC projecting 5-HT neurons. Red, tdTomato retrograde labeled neurons; green, anti-Tph2 staining neurons; orange, double stained neurons. Scale: 100 μm. (A_2) OXT potentiates glutamate synapses of DRN^{mPFC} 5-HT neurons. Upper panel illustrates sample eEPSC traces taken at time points indicated in lower panel. Scale bars: 50 pA, 25 ms. Lower panel is a summary graph of OXT-induced potentiation of eEPSC amplitude (●, n = 6, p = 0.0013). (A_3) OXT inhibits glutamate synapses of DRN^{mPFC} 5-HT neurons. Upper panel illustrates sample eEPSC traces taken at time points indicated in lower panel. Scale bars: 50 pA, 25 ms. Lower graph is a summary of OXT-induced inhibition of eEPSC amplitude (●, n = 6, p = 0.0032).

(B_1) Fluorescence images showing LHb projecting DRN 5-HT neurons. Red, tdTomato retrograde labeled neurons; green, anti-Tph2 staining neurons; orange, double stained neurons. Scale: 100 μm. (B_2) OXT inhibits glutamate synapses of

Figure 6. *Continued*

DRN^{LHb} 5-HT neurons. Upper panel illustrates sample eEPSC traces taken at time points indicated in lower panel. Lower graph depicts a summary of OXT-induced depression of eEPSC amplitude (●, n = 5, p = 0.0114). (C_1) Fluorescence image of showing DRN^{CeA} projecting neurons. Red, tdTomato retrograde labeled neurons; green, anti-Tph2 staining neurons; orange, double stained neurons. Scale: 100 μm. (C_2) OXT inhibits glutamate synapses of DRN^{CeA} 5-HT neurons. Upper panel illustrates sample eEPSC traces taken at time points indicated in lower panel. Lower graph is a summary of the averaged effect of OXT on eEPSC amplitude (●, n = 7, p = 0.0017).

Target-specific gating of DRN glutamate synapses by OXT

Accumulating evidence indicate that DRN 5-HT neurons are heterogeneous neurons clustered in different subpopulations with specific physiological and molecular properties.[57–59] Each subgroup of 5-HT neurons preferentially project to distinct brain targets and mediate specific physiological functions.[60,61] This raises the possibility that glutamate synapses of various subsets of DRN 5-HT projecting neurons may be differentially modulated by OXT. To test this possibility, we examined the effects of OXT on glutamate synapses of 5-HT neurons projecting to the medial prefrontal cortex (DRN^{mPFC}), the lateral habenula (DRN^{LHb}) and the central amygdala (DRN^{CeA}), which are known to regulate stress homeostasis.[62–64] We first targeted DRN^{mPFC} neurons by injecting retrograde adeno-associated virus (AAV) expressing tdTomato (rgAAV-CAG-tdTomato) in the prelimbic (PL) and infralimbic (IL) subregions of the mPFC and performed whole-cell recordings from retrogradely labeled DRN neurons. Consistent with earlier reports,[58,65] we found that tdTomato-labeled DRN^{mPFC} neurons were mainly clustered in the vmDRN between the medial longitudinal fasciculus (mlf) (Figure 6A_1). Co-immunostaining of DRN sections for tryptophan hydroxylase 2 (Tph2) revealed that the vast majority (85.5 ± 10.5%) of DRN tdTomato labeled neurons were also Tph2 positive (Figure 6A_1). Whole-cell recordings from these neurons showed that OXT (1 μM) potentiated (158.74 ± 8.88% of baseline, n = 6, p = 0.0013 vs. baseline, Figure 6A_2) and depressed (75.50 ± 4.83 of baseline, n = 6, p = 0.0032 vs. baseline, Figure 6A_3) the amplitude of eEPSCs in 80% and 20% of these neurons, respectively, indicating that OXTRs preferentially potentiate glutamate synapses of DRN^{mPFC} neurons.

Next, using similar approach, we targeted DRN^{LHb} and DRN^{CeA} neurons. We found that dtTomato-labeled DRN^{LHb} neurons were scattered throughout the dmDRn, vmDRn, and lateral wings (Figure 6B_1). Co-staining for Tph2 indicated that most of tdTomato neurons (76.6 ± 8.4%) were also Tph2 positive neurons (Figure 6B_1). In contrast, dtTomato-labeled DRN^{CeA} neurons were clustered in the vmDRN between the mlf, and most of these neurons were also Tph2 positive (82.01 ± 6.07%) (Figure 6C_1). Bath application of OXT (1 μM) depressed the amplitude of eEPSC in all DRN^{LHb} (56.49 ± 9.81% of baseline, n = 5, p = 0.0114 vs. baseline, Figure 6B_2) and DRN^{CeA} neurons (68.04 ± 6.09% of baseline, n = 7, p = 0.0017 vs. baseline, Figure 6C_2), thereby indicating that glutamate synapses of these neurons are mainly inhibited by OXTRs.

DISCUSSION

The hormone OXT controls wide spectrum of socially driven behaviors via modulation of central 5-HT system. Dysfunctions of both OXT and 5-HT systems contribute to social and emotional deficits associated with neurodevelopmental disorders, such as autism spectrum disorder (ASD).[29,31,32] However, the precise cellular mechanisms by which OXT regulates the function of DRN 5-HT neurons are not known. Here, we show that OXT via activation of OXTRs excites and alters the firing pattern of DRN 5-HT neurons. Beside these postsynaptic effects, our study reveals that OXT exerts target-specific gating of excitatory synaptic inputs to DRN by preferentially potentiating glutamate synapses of DRN^{mPFC} neurons while inhibiting those impinging onto DRN^{LHb} and DRN^{CeA} neurons. The depression and potentiation of DRN glutamate synapses are signaled by two distinct retrograde lipid messengers, 2-AG and AA, respectively. As such, the present study unravels the cellular mechanisms by which OXT controls the function of DRN 5-HT neurons.

The distribution pattern of OXTRs and oxytocinergic fibers in the DRN supports a key role of OXT in modulating DRN 5-HT neurons, which are implicated in the regulation of social and emotional behaviors.[14,66,67] Indeed, the present study reveals that OXT robustly enhances the spontaneous activity and depolarizes DRN 5-HT neurons. These excitatory effects are readily blocked by OXTR antagonist and by inhibiting postsynaptic G-proteins demonstrating that they are mediated by activation of postsynaptic OXTRs. Interestingly, activation of these receptors has also been shown to depolarize and increase neuronal excitability in various brain areas, such as, the CA2 region of the hippocampus,[68] the subiculum,[69] and the lateral

amygdala,[70] thereby indicating that OXT largely exerts postsynaptic excitatory effects in the brain. In addition to the increased intrinsic excitability, OXT transforms firing pattern of putative DRN 5-HT neurons from regular to bursting activity. A similar effect has also been reported in CA2 pyramidal neurons.[68] Most of DRN 5-HT neurons are quiescent or fire at slow and regular frequency,[36,37] and the probability to encounter burst firing neurons in the DRN is very low.[71] The OXT-induced switch from low regular to high burst firing mode combined with the increased excitability could mediate the reported *in vivo* increase of 5-HT release and contribute, at least in part, to anxiolytic-like effects induced by activation of OXTRs.[13,72] Furthermore, because activation of DRN 5-HT neurons increases sociability,[30,66] it is possible that the OXT-induced excitation of these neurons could encode the prosocial effects of OXT, though additional studies are required to directly test this notion.

Along with the increased intrinsic excitability, OXT bidirectionally controls the strength of glutamate synapses of putative DRN 5-HT neurons. Depending on the subpopulation of 5-HT neurons, OXT can either depress or potentiate glutamate synapses via a decrease and increase in glutamate release, respectively. The OXT-induced decrease in glutamate release is consistent with previous studies showing that OXT presynaptically inhibits glutamatergic transmission in others brain areas.[23,73,74] Mechanistically, the current study reveals that the OXT-induced depression of DRN glutamate synapses is prevented by inhibiting postsynaptic G-proteins, by blocking CB1Rs and by inhibiting PLC/DAGL cascade. These findings indicate that OXT inhibits glutamatergic transmission onto putative DRN 5-HT neurons via retrograde 2-AG signaling, an eCB known to controls the strength and plasticity of DRN glutamate synapses.[75] Such conclusion agrees with numerous studies showing that OXTR are canonically coupled to $G\alpha_{q/11}$-G-protein-coupled receptors[42,76] and with the notion that activation of these receptors increases the synthesis and release of 2-AG in several brain areas,[40,77,78] including DRN.[39] The finding that OXTRs inhibit the strength of glutamate synapses by recruiting retrograde eCB signaling reveals a functional link between OXT and eCB systems that could play a key role in mediating the behavior and physiological effects of OXT. Consistent with this concept, results from a previous study have shown that OXT enhances social reward, at least in apart, via a recruitment of brain eCB signaling.[79]

In a subset of putative DRN 5-HT neurons, activation of postsynaptic OXTRs potentiates glutamatergic transmission by enhancing glutamate release. This effect is not signaled by PLC/DAGL, but rather by activation of $cPLA_2$/AA signaling cascade. The released AA retrogradely increases glutamate release by inhibiting voltage-gated A potassium channels (Figure 8). Several lines of evidence support this model. First, the OXT-induced potentiation of excitatory transmission is blocked by inhibiting postsynaptic G-protein function and $cPLA_2$, but not PLC/DAGL signaling cascade. Second, manipulation that increases AA levels enhances glutamatergic transmission and mimics the effect of OXT. Finally, pharmacological blockade of voltage-dependent potassium channels mimics the OXT-induced increase in glutamate release and prevents additional potentiation of DRN glutamate synapses. While prior 4-AP application might not occlude any further effect of OXT in facilitating glutamate release, these results suggest their common mechanism and the direct involvement of AA and A-type potassium channels. Interestingly, such a functional model is consistent with previous studies showing that exogenous AA directly inhibits A-type potassium channels[51,52,80] and potentiates glutamatergic transmission.[80,81] Consequently, the current finding further supports the synaptic role of AA and suggest that OXTR-driven AA release serves as a retrograde messenger that gates synaptic transmission in the DRN. Given that OXTRs and $cPLA_2$ are expressed in neurons of many others brain regions, it is possible that OXTR-driven AA signaling may be a general mechanism by which OXT potentiates central synapses.

Altogether, our findings indicate that by engaging different membrane lipids (i.e. 2-AG, AA), OXT can bidirectionally control excitatory inputs to DRN 5-HT neurons. This control is target-specific, as OXT preferentially potentiates glutamatergic inputs to DRN^{mPFC} neurons, while inhibiting the inputs to DRN^{LHb} and DRN^{CeA} neurons. Although the precise physiological roles of OXT-mediated bidirectional and target-specific synaptic gating in the DRN remain unknown, it is possible that, OXT serves as a filter that engage a specific set of neuronal circuits to encode complex social behaviors. In addition, given the involvement of DRN 5-HT system in effecting regulation[67,82] and sociability,[30] the new evidence of OXT-mediated control of the excitability of 5-HT neurons and synaptic dynamic in the DRN may represent a potential neuronal mechanism by which OXT modulates social and emotional behaviors. Consistent with this notion, results from both animal and human studies have shown that OXT ameliorates social deficits in ASD via activation of 5-HT system.[23,33–35,83] Furthermore, growing evidence indicate that eCB system regulates social

behaviors[79,84] and that enhancing eCB signaling rescues social deficits observed in various animal models of ASD.[79,85] The present finding that OXT regulates synaptic dynamic in the DRN by recruiting eCB signaling may represents an additional mechanism by which OXT control plethora of behaviors and physiological functions. Consequently, OXT-driven eCB signaling in the DRN could represent a target for future treatment strategies of social and emotional deficits associated with neurodevelopment disorders.

Limitations of the study

In this study, we show that OXT plays a key role in controlling the excitability of putative DRN 5-HT neurons and gating their glutamate synapses. Although our results unravel a cell-type-specific bidirectional control of DRN glutamate synapses, future studies using molecularly identified subset of DRN 5-HT neurons, combined with channelrhodopsin assisted circuit analysis, are required to further decipher the effects of OXT on the various DRN neuronal circuitries.

STAR★METHODS

Detailed methods are provided in the online version of this paper and include the following:

- KEY RESOURCES TABLE
- RESOURCE AVAILABILITY
  - Lead contact
  - Materials availability
  - Data and code availability
- EXPERIMENTAL MODEL AND SUBJECT DETAILS
- METHOD DETAILS
  - *In vivo* viral injections
  - Ex-vivo electrophysiology
  - Immunohistochemistry
- QUANTIFICATION AND STATISTICAL ANALYSIS

ACKNOWLEDGMENTS

This work was supported by the National Institute of Mental Health grant MH122461.

AUTHOR CONTRIBUTIONS

S.O. performed electrophysiological experiments and wrote the initial draft. S.H.D. and S.O. designed the experiments and performed data analysis. R.Y.S. participated in the experimental and manuscript editing. S.H.D. wrote the manuscript.

DECLARATION OF INTERESTS

The authors declare no competing conflict of interest.

INCLUSION AND DIVERSITY

We support inclusive, diverse, and equitable conduct of research.

Received: February 20, 2023
Revised: March 20, 2023
Accepted: April 18, 2023
Published: April 23, 2023

REFERENCES

1. Blanks, A.M., and Thornton, S. (2003). The role of oxytocin in parturition. BJOG An Int. J. Obstet. Gynaecol. *110*, 46–51. https://doi.org/10.1016/S1470-0328(03)00024-7.

2. Soloff, M.S., Alexandrova, M., and Fernstrom, M.J. (1979). Oxytocin receptors: triggers for parturition and lactation. Science *204*, 1313–1315. https://doi.org/10.1126/science.221972.

3. Mohr, E., Schmitz, E., and Richter, D. (1988). A single rat genomic DNA fragment encodes both the oxytocin and vasopressin genes separated by 11 kilobases and oriented in opposite transcriptional directions. Biochimie *70*, 649–654. https://doi.org/10.1016/0300-9084(88)90249-0.

4. Zimmerman, E.A., Nilaver, G., Hou-Yu, A., and Silverman, A.J. (1984). Vasopressinergic and oxytocinergic pathways in the central nervous system. Fed. Proc. *43*, 91–96.

5. de Vries, G.J., and Buijs, R.M. (1983). The origin of the vasopressinergic and oxytocinergic innervation of the rat brain with special reference to the lateral septum. Brain Res. *273*, 307–317. https://doi.org/10.1016/0006-8993(83)90855-7.

6. Sofroniew, M.V. (1980). Projections from vasopressin, oxytocin, and neurophysin neurons to neural targets in the rat and human. J. Histochem. Cytochem. *28*, 475–478. https://doi.org/10.1177/28.5.7381192.

7. Zhang, K., Fan, Y., Yu, R., Tian, Y., Liu, J., and Gong, P. (2021). Intranasal oxytocin administration but not peripheral oxytocin regulates behaviors of attachment insecurity: a meta-analysis. Psychoneuroendocrinology *132*, 105369. https://doi.org/10.1016/j.psyneuen.2021.105369.

8. Menon, R., Grund, T., Zoicas, I., Althammer, F., Fiedler, D., Biermeier, V., Bosch, O.J., Hiraoka, Y., Nishimori, K., Eliava, M., et al. (2018). Oxytocin signaling in the lateral septum prevents social fear during lactation. Curr. Biol. *28*, 1066–1078.e6. https://doi.org/10.1016/j.cub.2018.02.044.

9. Knobloch, H.S., Charlet, A., Hoffmann, L.C., Eliava, M., Khrulev, S., Cetin, A.H., Osten, P., Schwarz, M.K., Seeburg, P.H., Stoop, R., and Grinevich, V. (2012). Evoked axonal oxytocin release in the central amygdala attenuates fear response. Neuron *73*, 553–566. https://doi.org/10.1016/j.neuron.2011.11.030.

10. Caffé, A.R., Van Ryen, P.C., Van Der Woude, T.P., and Van Leeuwen, F.W. (1989). Vasopressin and oxytocin systems in the brain and upper spinal cord of *Macaca fascicularis*: vasopressin and oxytocin in a primate CNS. J. Comp. Neurol. *287*, 302–325. https://doi.org/10.1002/cne.902870304.

11. Kimura, T., Tanizawa, O., Mori, K., Brownstein, M.J., and Okayama, H. (1992). Structure and expression of a human oxytocin receptor. Nature *356*, 526–529. https://doi.org/10.1038/356526a0.

12. Gimpl, G., and Fahrenholz, F. (2001). The oxytocin receptor system: structure, function, and regulation. Physiol. Rev. *81*, 629–683. https://doi.org/10.1152/physrev.2001.81.2.629.

13. Yoshimura, R., Kimura, T., Watanabe, D., and Kiyama, H. (1996). Differential expression of oxytocin receptor mRNA in the developing rat brain. Neurosci. Res. *24*, 291–304. https://doi.org/10.1016/0168-0102(95)01003-3.

14. Dölen, G. (2015). Oxytocin: parallel processing in the social brain? J. Neuroendocrinol. *27*, 516–535. https://doi.org/10.1111/jne.12284.

15. Ferguson, J.N., Young, L.J., Hearn, E.F., Matzuk, M.M., Insel, T.R., and Winslow, J.T. (2000). Social amnesia in mice lacking the oxytocin gene. Nat. Genet. *25*, 284–288. https://doi.org/10.1038/77040.

16. Takayanagi, Y., Yoshida, M., Bielsky, I.F., Ross, H.E., Kawamata, M., Onaka, T., Yanagisawa, T., Kimura, T., Matzuk, M.M., Young, L.J., and Nishimori, K. (2005). Pervasive social deficits, but normal parturition, in oxytocin receptor-deficient mice. Proc. Natl. Acad. Sci. *102*, 16096–16101. https://doi.org/10.1073/pnas.0505312102.

17. Waldherr, M., and Neumann, I.D. (2007). Centrally released oxytocin mediates mating-induced anxiolysis in male rats. Proc. Natl. Acad. Sci. *104*, 16681–16684. https://doi.org/10.1073/pnas.0705860104.

18. Lawson, E.A. (2017). The effects of oxytocin on eating behaviour and metabolism in humans. Nat. Rev. Endocrinol. *13*, 700–709. https://doi.org/10.1038/nrendo.2017.115.

19. Windle, R.J., Shanks, N., Lightman, S.L., and Ingram, C.D. (1997). Central oxytocin administration reduces stress-induced corticosterone release and anxiety behavior in rats [1]. Endocrinology *138*, 2829–2834. https://doi.org/10.1210/endo.138.7.5255.

20. Herpertz, S.C., Schmitgen, M.M., Fuchs, C., Roth, C., Wolf, R.C., Bertsch, K., Flor, H., Grinevich, V., and Boll, S. (2019). Oxytocin effects on pain perception and pain anticipation. J. Pain *20*, 1187–1198. https://doi.org/10.1016/j.jpain.2019.04.002.

21. Grieb, Z.A., and Lonstein, J.S. (2021). Oxytocin receptor expression in the midbrain dorsal raphe is dynamic across female reproduction in rats. J. Neuroendocrinol. *33*, e12926. https://doi.org/10.1111/jne.12926.

22. Yoshida, M., Takayanagi, Y., Inoue, K., Kimura, T., Young, L.J., Onaka, T., and Nishimori, K. (2009). Evidence that oxytocin exerts anxiolytic effects via oxytocin receptor expressed in serotonergic neurons in mice. J. Neurosci. *29*, 2259–2271. https://doi.org/10.1523/JNEUROSCI.5593-08.2009.

23. Dölen, G., Darvishzadeh, A., Huang, K.W., and Malenka, R.C. (2013). Social reward requires coordinated activity of nucleus accumbens oxytocin and serotonin. Nature *501*, 179–184. https://doi.org/10.1038/nature12518.

24. Calcagnoli, F., Stubbendorff, C., Meyer, N., de Boer, S.F., Althaus, M., and Koolhaas, J.M. (2015). Oxytocin microinjected into the central amygdaloid nuclei exerts anti-aggressive effects in male rats. Neuropharmacology *90*, 74–81. https://doi.org/10.1016/j.neuropharm.2014.11.012.

25. Pagani, J.H., Williams Avram, S.K., Cui, Z., Song, J., Mezey, É., Senerth, J.M., Baumann, M.H., and Young, W.S. (2015). Raphe serotonin neuron-specific oxytocin receptor knockout reduces aggression without affecting anxiety-like behavior in male mice only: 5-HT Oxtr KO decouples aggression from anxiety. Genes Brain Behav. *14*, 167–176. https://doi.org/10.1111/gbb.12202.

26. Figueira, R.J., Peabody, M.F., and Lonstein, J.S. (2008). Oxytocin receptor activity in the ventrocaudal periaqueductal gray modulates anxiety-related behavior in postpartum rats. Behav. Neurosci. *122*, 618–628. https://doi.org/10.1037/0735-7044.122.3.618.

27. Van de Kar, L.D., Javed, A., Zhang, Y., Serres, F., Raap, D.K., and Gray, T.S. (2001). 5-HT $_{2A}$ receptors stimulate ACTH, corticosterone, oxytocin, renin, and prolactin release and activate hypothalamic CRF and oxytocin-expressing cells. J. Neurosci. *21*, 3572–3579. https://doi.org/10.1523/JNEUROSCI.21-10-03572.2001.

28. Ho, S.S.N., Chow, B.K.C., and Yung, W.-H. (2007). Serotonin increases the excitability of the hypothalamic paraventricular nucleus magnocellular neurons: serotonin excites PVN magnocellular neurons. Eur. J. Neurosci. *25*, 2991–3000. https://doi.org/10.1111/j.1460-9568.2007.05547.x.

29. Muller, C.L., Anacker, A.M.J., and Veenstra-VanderWeele, J. (2016). The serotonin system in autism spectrum disorder: from biomarker to animal models. Neuroscience *321*, 24–41. https://doi.org/10.1016/j.neuroscience.2015.11.010.

30. Walsh, R.J., Krabbendam, L., Dewinter, J., and Begeer, S. (2018). Brief report: gender identity differences in autistic adults: associations with perceptual and socio-cognitive profiles. J. Autism Dev. Disord. *48*, 4070–4078. https://doi.org/10.1007/s10803-018-3702-y.

31. Hörnberg, H., Pérez-Garci, E., Schreiner, D., Hatstatt-Burklé, L., Magara, F., Baudouin, S., Matter, A., Nacro, K., Pecho-Vrieseling, E., and Scheiffele, P. (2020). Rescue of oxytocin response and social behaviour in a mouse model of autism. Nature *584*, 252–256. https://doi.org/10.1038/s41586-020-2563-7.

32. Quattrocki, E., and Friston, K. (2014). Autism, oxytocin and interoception. Neurosci. Biobehav. Rev. *47*, 410–430. https://doi.org/10.1016/j.neubiorev.2014.09.012.

33. Lefevre, A., Richard, N., Jazayeri, M., Beuriat, P.-A., Fieux, S., Zimmer, L., Duhamel, J.-R., and Sirigu, A. (2017). Oxytocin and serotonin brain mechanisms in the nonhuman primate. J. Neurosci. *37*, 6741–6750. https://doi.org/10.1523/JNEUROSCI.0659-17.2017.

34. Mottolese, R., Redouté, J., Costes, N., Le Bars, D., and Sirigu, A. (2014). Switching brain serotonin with oxytocin. Proc. Natl. Acad. Sci. *111*, 8637–8642. https://doi.org/10.1073/pnas.1319810111.

35. Nagano, M., Takumi, T., and Suzuki, H. (2018). Critical roles of serotonin-oxytocin interaction during the neonatal period in social behavior in 15q dup mice with autistic traits. Sci. Rep. *8*, 13675. https://doi.org/10.1038/s41598-018-32042-9.

36. Haj-Dahmane, S. (2001). D $_2$ -like dopamine receptor activation excites rat dorsal raphe 5-HT neurons *in vitro*: dopaminergic excitation of DRN 5-HT neurons. Eur. J. Neurosci. *14*, 125–134. https://doi.org/10.1046/j.0953-816x.2001.01616.x.

37. Vandermaelen, C.P., and Aghajanian, G.K. (1983). Electrophysiological and Pharmacological Characterization of Serotonergic Dorsal Raphe Neurons Recorded Extracellularly and Intracellularly in Rat Brain Slices.

38. Geddes, S.D., Assadzada, S., Lemelin, D., Sokolovski, A., Bergeron, R., Haj-Dahmane, S., and Béïque, J.C. (2016). Target-specific

modulation of the descending prefrontal cortex inputs to the dorsal raphe nucleus by cannabinoids. Proc. Natl. Acad. Sci. *113*, 5429–5434. https://doi.org/10.1073/pnas.1522754113.

39. Haj-Dahmane, S., and Shen, R.Y. (2005). The wake-promoting peptide orexin-B inhibits glutamatergic transmission to dorsal raphe nucleus serotonin neurons through retrograde endocannabinoid signaling. J. Neurosci. *25*, 896–905. https://doi.org/10.1523/JNEUROSCI.3258-04.2005.

40. Ohno-Shosaku, T., Matsui, M., Fukudome, Y., Shosaku, J., Tsubokawa, H., Taketo, M.M., Manabe, T., and Kano, M. (2003). Postsynaptic M1 and M3 receptors are responsible for the muscarinic enhancement of retrograde endocannabinoid signalling in the hippocampus. Eur. J. Neurosci. *18*, 109–116. https://doi.org/10.1046/j.1460-9568.2003.02732.x.

41. Jurek, B., and Neumann, I.D. (2018). The oxytocin receptor: from intracellular signaling to behavior. Physiol. Rev. *98*, 1805–1908.

42. Ku, C.Y., Qian, A., Wen, Y., Anwer, K., and Sanborn, B.M. (1995). Oxytocin stimulates myometrial guanosine triphosphatase and phospholipase-C activities via coupling to G alpha q/11. Endocrinology *136*, 1509–1515. https://doi.org/10.1210/endo.136.4.7895660.

43. Bisogno, T., Howell, F., Williams, G., Minassi, A., Cascio, M.G., Ligresti, A., Matias, I., Schiano-Moriello, A., Paul, P., Williams, E.-J., et al. (2003). Cloning of the first sn1-DAG lipases points to the spatial and temporal regulation of endocannabinoid signaling in the brain. J. Cell Biol. *163*, 463–468. https://doi.org/10.1083/jcb.200305129.

44. Tanimura, A., Yamazaki, M., Hashimotodani, Y., Uchigashima, M., Kawata, S., Abe, M., Kita, Y., Hashimoto, K., Shimizu, T., Watanabe, M., et al. (2010). The endocannabinoid 2-arachidonoylglycerol produced by diacylglycerol lipase α mediates retrograde suppression of synaptic transmission. Neuron *65*, 320–327. https://doi.org/10.1016/j.neuron.2010.01.021.

45. Silvia, W.J., and Homanics, G.E. (1988). Role of phospholipase C in mediating oxytocin -induced release of prostaglandin F2α from ovine endometrial tissue. Prostaglandins *35*, 535–548. https://doi.org/10.1016/0090-6980(88)90029-9.

46. Burns, P.D., Graf, G.A., Hayes, S.H., and Silvia, W.J. (2000). Effect of oxytocin on expression of cytosolic phospholipase A2 mRNA and protein in ovine endometrial tissue in vivo. Domest. Anim. Endocrinol. *19*, 237–246.

47. Farina, M.G., Billi, S., Leguizamón, G., Weissmann, C., Guadagnoli, T., Ribeiro, M.L., and Franchi, A.M. (2007). Secretory and cytosolic phospholipase A2 activities and expression are regulated by oxytocin and estradiol during labor. Reproduction *134*, 355–364. https://doi.org/10.1530/REP-07-0078.

48. Breder, C.D., Dewitt, D., and Kraig, R.P. (1995). Characterization of inducible cyclooxygenase in rat brain. J. Comp. Neurol. *355*, 296–315. https://doi.org/10.1002/cne.903550208.

49. Yagami, T., Yamamoto, Y., and Koma, H. (2017). 15-deoxy-Δ12,14-prostaglandin J2 in neurodegenerative diseases and cancers. Oncotarget *8*, 9007–9008. https://doi.org/10.18632/oncotarget.14701.

50. Nakamura, K., Kaneko, T., Yamashita, Y., Hasegawa, H., Katoh, H., and Negishi, M. (2000). Immunohistochemical localization of prostaglandin EP3 receptor in the rat nervous system. J. Comp. Neurol. *421*, 543–569. https://doi.org/10.1002/(SICI)1096-9861(20000612)421:4<543::AID-CNE6>3.0.CO;2-3.

51. Keros, S., and McBain, C.J. (1997). Arachidonic acid inhibits transient potassium currents and broadens action potentials during electrographic seizures in hippocampal pyramidal and inhibitory interneurons. J. Neurosci. *17*, 3476–3487. https://doi.org/10.1523/JNEUROSCI.17-10-03476.1997.

52. Villarroel, A., and Schwarz, T.L. (1996). Inhibition of the Kv4 (Shal) family of transient K+ currents by arachidonic acid. J. Neurosci. *16*, 1016–1025. https://doi.org/10.1523/JNEUROSCI.16-03-01016.1996.

53. Angelova, P.R., and Müller, W.S. (2009). Arachidonic acid potently inhibits both postsynaptic-type Kv4.2 and presynaptic-type Kv1.4 I_A potassium channels. Eur. J. Neurosci. *29*, 1943–1950. https://doi.org/10.1111/j.1460-9568.2009.06737.x.

54. Devor, D.C., and Frizzell, R.A. (1998). Modulation of K^+ channels by arachidonic acid in T84 cells. I. Inhibition of the Ca^{2+} -dependent K^+ channel. Am. J. Physiol. *274*, C138–C148. https://doi.org/10.1152/ajpcell.1998.274.1.C138.

55. Meves, H. (1994). Arachidonic acid a potassium channels. Prog. Neurobiol. *43*, 175–186.

56. Cooper, E.C., Milroy, A., Jan, Y.N., Jan, L.Y., and Lowenstein, D.H. (1998). Presynaptic localization of Kv1.4-containing A-type potassium channels near excitatory synapses in the Hippocampus. J. Neurosci. *18*, 965–974. https://doi.org/10.1523/JNEUROSCI.18-03-00965.1998.

57. Okaty, B.W., Freret, M.E., Rood, B.D., Brust, R.D., Hennessy, M.L., deBairos, D., Kim, J.C., Cook, M.N., and Dymecki, S.M. (2015). Multi-scale molecular deconstruction of the serotonin neuron system. Neuron *88*, 774–791. https://doi.org/10.1016/j.neuron.2015.10.007.

58. Fernandez, S.P., Cauli, B., Cabezas, C., Muzerelle, A., Poncer, J.-C., and Gaspar, P. (2016). Multiscale single-cell analysis reveals unique phenotypes of raphe 5-HT neurons projecting to the forebrain. Brain Struct. Funct. *221*, 4007–4025. https://doi.org/10.1007/s00429-015-1142-4.

59. Andrade, R., and Haj-Dahmane, S. (2013). Serotonin neuron diversity in the dorsal raphe. ACS Chem. Neurosci. *4*, 22–25. https://doi.org/10.1021/cn300224n.

60. Waselus, M., Valentino, R.J., and Van Bockstaele, E.J. (2011). Collateralized dorsal raphe nucleus projections: a mechanism for the integration of diverse functions during stress. J. Chem. Neuroanat. *41*, 266–280. https://doi.org/10.1016/j.jchemneu.2011.05.011.

61. Muzerelle, A., Scotto-Lomassese, S., Bernard, J.F., Soiza-Reilly, M., and Gaspar, P. (2016). Conditional anterograde tracing reveals distinct targeting of individual serotonin cell groups (B5–B9) to the forebrain and brainstem. Brain Struct. Funct. *221*, 535–561. https://doi.org/10.1007/s00429-014-0924-4.

62. Amat, J., Baratta, M.V., Paul, E., Bland, S.T., Watkins, L.R., and Maier, S.F. (2005). Medial prefrontal cortex determines how stressor controllability affects behavior and dorsal raphe nucleus. Nat. Neurosci. *8*, 365–371. https://doi.org/10.1038/nn1399.

63. Hassell, J.E., Collins, V.E., Li, H., Rogers, J.T., Austin, R.C., Visceau, C., Nguyen, K.T., Orchinik, M., Lowry, C.A., and Renner, K.J. (2019). Local inhibition of uptake2 transporters augments stress-induced increases in serotonin in the rat central amygdala. Neurosci. Lett. *701*, 119–124. https://doi.org/10.1016/j.neulet.2019.02.022.

64. Baker, P.M., Mathis, V., Lecourtier, L., Simmons, S.C., Nugent, F.S., Hill, S., and Mizumori, S.J.Y. (2022). Lateral habenula beyond avoidance: roles in stress, memory, and decision-making with implications for psychiatric disorders. Front. Syst. Neurosci. *16*, 826475. https://doi.org/10.3389/fnsys.2022.826475.

65. Prouty, E.W., Chandler, D.J., and Waterhouse, B.D. (2017). Neurochemical differences between target-specific populations of rat dorsal raphe projection neurons. Brain Res. *1675*, 28–40. https://doi.org/10.1016/j.brainres.2017.08.031.

66. Li, T., Jia, S.-W., Hou, D., Liu, X., Li, D., Liu, Y., Cui, D., Wang, X., Hou, C., Brown, C.H., and Wang, Y.F. (2021). Intranasal oxytocin restores maternal behavior and oxytocin neuronal activity in the supraoptic nucleus in rat dams with cesarean delivery. Neuroscience *468*, 235–246. https://doi.org/10.1016/j.neuroscience.2021.06.020.

67. Ren, J., Friedmann, D., Xiong, J., Liu, C.D., Ferguson, B.R., Weerakkody, T., DeLoach, K.E., Ran, C., Pun, A., Sun, Y., et al. (2018). Anatomically defined and functionally distinct dorsal raphe serotonin sub-systems. Cell *175*, 472–487.e20. https://doi.org/10.1016/j.cell.2018.07.043.

68. Tirko, N.N., Eyring, K.W., Carcea, I., Mitre, M., Chao, M.V., Froemke, R.C., and Tsien, R.W. (2018). Oxytocin transforms firing mode of CA2 hippocampal neurons. Neuron *100*, 593–608.e3. https://doi.org/10.1016/j.neuron.2018.09.008.

69. Hu, B., Boyle, C.A., and Lei, S. (2021). Activation of oxytocin receptors excites subicular neurons by multiple signaling and ionic mechanisms. Cereb. Cortex *31*, 2402–2415. https://doi.org/10.1093/cercor/bhaa363.

70. Crane, N.A., Chang, F., Kinney, K.L., and Klumpp, H. (2021). Individual differences in striatal and amygdala response to emotional faces are related to symptom severity in social anxiety disorder. Neuroimage. Clin. *30*, 102615. https://doi.org/10.1016/j.nicl.2021.102615.

71. Hajós, M., Allers, K.A., Jennings, K., Sharp, T., Charette, G., Sík, A., and Kocsis, B. (2007). Neurochemical identification of stereotypic burst-firing neurons in the rat dorsal raphe nucleus using juxtacellular labelling methods: burst firing 5-HT neurons. Eur. J. Neurosci. *25*, 119–126. https://doi.org/10.1111/j.1460-9568.2006.05276.x.

72. Ring, R.H., Malberg, J.E., Potestio, L., Ping, J., Boikess, S., Luo, B., Schechter, L.E., Rizzo, S., Rahman, Z., and Rosenzweig-Lipson, S. (2006). Anxiolytic-like activity of oxytocin in male mice: behavioral and autonomic evidence, therapeutic implications. Psychopharmacology (Berl.) *185*, 218–225. https://doi.org/10.1007/s00213-005-0293-z.

73. Kombian, S.B., Mouginot, D., and Pittman, Q.J. (1997). Dendritically released peptides act as retrograde modulators of afferent excitation in the supraoptic nucleus in vitro. Neuron *19*, 903–912. https://doi.org/10.1016/S0896-6273(00)80971-X.

74. Ninan, I. (2011). Oxytocin suppresses basal glutamatergic transmission but facilitates activity-dependent synaptic potentiation in the medial prefrontal cortex: oxytocin facilitates synaptic potentiation in the prefrontal cortex. J. Neurochem. *119*, 324–331. https://doi.org/10.1111/j.1471-4159.2011.07430.x.

75. Haj-Dahmane, S., and Shen, R.-Y. (2009). Endocannabinoids suppress excitatory synaptic transmission to dorsal raphe serotonin neurons through the activation of presynaptic CB $_1$ receptors. J. Pharmacol. Exp. Ther. *331*, 186–196. https://doi.org/10.1124/jpet.109.153858.

76. Grinevich, V., Knobloch-Bollmann, H.S., Eliava, M., Busnelli, M., and Chini, B. (2016). Assembling the puzzle: pathways of oxytocin signaling in the brain. Biol. Psychiatry *79*, 155–164. https://doi.org/10.1016/j.biopsych.2015.04.013.

77. Maejima, T., Hashimoto, K., Yoshida, T., Aiba, A., and Kano, M. (2001). Presynaptic inhibition caused by retrograde signal from metabotropic glutamate to cannabinoid receptors. Neuron *31*, 463–475. https://doi.org/10.1016/S0896-6273(01)00375-0.

78. Xiao, L., Priest, M.F., and Kozorovitskiy, Y. (2018). Oxytocin functions as a spatiotemporal filter for excitatory synaptic inputs to VTA dopamine neurons. Elife *7*, e33892. https://doi.org/10.7554/eLife.33892.

79. Wei, D., Dinh, D., Lee, D., Li, D., Anguren, A., Moreno-Sanz, G., Gall, C.M., and Piomelli, D. (2016). Enhancement of anandamide-mediated endocannabinoid signaling corrects autism-related social impairment. Cannabis Cannabinoid Res. *1*, 81–89. https://doi.org/10.1089/can.2015.0008.

80. Carta, M., Lanore, F., Rebola, N., Szabo, Z., Da Silva, S.V., Lourenço, J., Verraes, A., Nadler, A., Schultz, C., Blanchet, C., and Mulle, C. (2014). Membrane lipids tune synaptic transmission by direct modulation of presynaptic potassium channels. Neuron *81*, 787–799. https://doi.org/10.1016/j.neuron.2013.12.028.

81. Drapeau, C., Pellerin, L., Wolfe, L.S., and Avoli, M. (1990). Long-term changes of synaptic transmission induced by arachidonic acid in the CA1 subfield of the rat hippocampus. Neurosci. Lett. *115*, 286–292. https://doi.org/10.1016/0304-3940(90)90470-T.

82. Teissier, A., Chemiakine, A., Inbar, B., Bagchi, S., Ray, R.S., Palmiter, R.D., Dymecki, S.M., Moore, H., and Ansorge, M.S. (2015). Activity of raphé serotonergic neurons controls emotional behaviors. Cell Rep. *13*, 1965–1976. https://doi.org/10.1016/j.celrep.2015.10.061.

83. Fukai, M., Hirosawa, T., Kikuchi, M., Ouchi, Y., Takahashi, T., Yoshimura, Y., Miyagishi, Y., Kosaka, H., Yokokura, M., Yoshikawa, E., et al. (2017). Oxytocin effects on emotional response to others' faces via serotonin system in autism: a pilot study. Psychiatry Res. Neuroimaging. *267*, 45–50. https://doi.org/10.1016/j.pscychresns.2017.06.015.

84. Litvin, Y., Phan, A., Hill, M.N., Pfaff, D.W., and McEwen, B.S. (2013). CB $_1$ receptor signaling regulates social anxiety and memory: CB1 receptor signaling regulates social anxiety and memory. Genes Brain Behav. *12*, 479–489. https://doi.org/10.1111/gbb.12045.

85. Wu, Y., Liu, Q., Guo, B., Ye, F., Ge, J., and Xue, L. (2020). BDNF activates postsynaptic TrkB receptors to induce endocannabinoid release and inhibit presynaptic calcium influx at a calyx-type synapse. J. Neurosci. *40*, 8070–8087. https://doi.org/10.1523/JNEUROSCI.2838-19.2020.

STAR★METHODS

KEY RESOURCES TABLE

REAGENT or RESOURCE	SOURCE	IDENTIFIER
Antibodies		
Mouse anti-Tph2	Abcam	ab211528
rabbit anti-RFP	Rockland	Ref# 600-401-379
Goat anti-mouse Alexa 488	Abcam	ab150113
Goat anti-rabbit Alexa 594	Abcam	ab150080
Bacterial and virus strains		
rgAAV-CAG-tdTomato	Addgene	cat # 59462
Experimental models: Organism/strains		
Male Sprague Dawley rats	Envigo	https://www.envigo.com/
Chemicals, peptides, and recombinant proteins		
NaCl	Fisher Scientific	CAS # 7647-14-5
Choline-Cl	Fisher Scientific	CAS # 1879-5008
CaCl2	Fisher Scientific	CAS # 10035-04-8
MgSO4	Fisher Scientific	CAS # 10034-99-8
KCl	Fisher Scientific	CAS # 7447-40-7
NaH2PO4	Fisher Scientific	CAS # 10049-21-5
NaHCO3	Fisher Scientific	CAS # 144-55-8
Glucose	Fisher Scientific	CAS # 50-99-7
Sodium L-ascorbate	Acros Organics	AC352685000
Sodium pyruvate	Sigma-Aldrich	CAS # 113-24-6
Oxytocin acetate salt	Bachem	CAS # 50-56-6
(Thr^4,Gly^7)-Oxytocin	Bachem	CAS # 60786-59-6
(d(CH$_2$)$_5^1$,Tyr(Me)^2,Orn^8)-Oxytocin trifluoroacetate salt	Bachem	CAS # 77327-45-8
AM251	Tocris Biosciences	Cat. No. 1117
U73122	Tocris Biosciences	Cat. No. 1268
U73343	Tocris Biosciences	Cat. No. 4133
RHC80267	Tocris Biosciences	Cat. No. 1842/10
AACOCCF3	Hellobio	HB2354
Arachidonic acid	Sigma-Aldrich	CAS # 506-32-1
NS393	Sigma-Aldrich	CAS # 123653-11-2
picrotoxin	Sigma-Aldrich	CAS # 124-87-8
Software and algorithms		
pClamp software	Molecular Devices	v10.7
Origin software	OriginLab Co	v8.0
Clampfit software	Molecular Devices	v10.7
CorelDRAW Graphics Suite	Coreldraw	v 2019
Other		
KOPF instruments	Tujunga	https://kopfinstruments.com/
Stoelting pump	Stoelting Co	https://stoeltingco.com/
Vibratome Leica	Leica Biosystem	VT1200S
Olympus BX51 microscope	Molecular Devices	https://www.moleculardevices.com/

(*Continued on next page*)

Continued

REAGENT or RESOURCE	SOURCE	IDENTIFIER
Multiclamp 700B amplifier	Molecular Devices	https://www.moleculardevices.com/
Digidata 1440	Molecular Devices	https://www.moleculardevices.com/
Microtome	American Optical	860 model

RESOURCE AVAILABILITY

Lead contact

Samir Haj-Dahmane: sh38@buffalo.edu.

Materials availability

Further information and request for resources are available from the lead contact upon request.

Data and code availability

- All raw data in this publication will be shared upon request.
- This paper does not report original code.
- Data reported in this paper or any additional information will be shared by the lead contact upon request.

EXPERIMENTAL MODEL AND SUBJECT DETAILS

All experiments and animal procedures used in this study were approved by the University at Buffalo Animal Care and Use Committee (IACUC) in accordance with the National Institutes of Health (NIH) Guideline for the Care and Use of Laboratory Animals. Male Sprague Dawley rats (4-7 weeks old) were kept in 12/12 h dark/light cycles with food and water ad libido at room temperature and standard humidity.

METHOD DETAILS

In vivo viral injections

For neuronal retrograde labeling, a retrograde tracer rgAAV-CAG-tdTomato (Addgene cat # 59462, Addgene, Watertown, MA, USA) was used. The viral particles were injected in the prelimbic and infralimbic areas of the mPFC, in the central amygdala (CeA) or lateral Habenula (LHb) of male Sprague Dawley rats (3 to 4 weeks) under ketamine (60 mg/kg) and xylazine (2.5 mg/kg) anesthesia. Briefly, rats were positioned in stereotaxic frame (KOPF instruments, Tujunga, CA, USA) and small burr holes were drilled above the brain regions of interest. The viral suspension was bilaterally injected either in the medial prefrontal cortex (mPFC) (coordinates to bregma: AP+3, ML $\pm$ 0.6, DV -4 to brain surface: 500 nl/side, 100 nl/min), the (coordinates to bregma: AP-2, ML $\pm$ 4, DV -8 to brain surface: 300 nl/side, 100 nl/min), or (coordinates to bregma: AP-3.6, ML $\pm$ 0.6, DV -4.6 to brain surface: 300 nl/side, 100 nl/min). The injections were performed using a 33-gauge needle attached to 5 µl syringe (Hamilton, Reno, NV, USA) and driven by a Stoelting pump (Stoelting Co, Wood Dale, IL, USA). After the injections were completed, animals were allowed to recover on the heat pad in their home cage. Animal welfare was monitored daily after the procedure. Two to three weeks after surgery, rats were used for *in vitro* electrophysiological and immunohistochemical studies.

Ex-vivo electrophysiology

To generate coronal brain slices containing the DRN, rats were deeply anesthetized by isoflurane and decapitated using guillotine, the brain was removed and brainstem region containing the DRN was isolated and sliced (350 µm) using a vibratome (Leica VT1200S; Leica Biosystem, St Louis, MO, USA) in ice-cold cutting solution of the following composition (in mM): 110 Choline-Cl; 2.5 KCl; 0.5 $CaCl_2$; 7 $MgSO_4$; 1.25 NaH_2PO_4; 26.2 $NaHCO_3$; 11.6 sodium L-ascorbate; 3.1 sodium pyruvate, 25 glucose and saturated with 95% O_2/5% CO_2. Slices were incubated in the cutting solution for 15 min at 35°C and then in regular ACSF of the following compositing (in mM: 119 NaCl; 2.5 $CaCl_2$; 1.3 $MgSO_4$; 1 NaH_2PO_4; 26.2 $NaHCO_3$; 11 glucose and continuously bubbled with a mixture of 95% O_2/5% CO_2) for 30 min at 35°C. After recovery,

slices were stored in holding chamber containing regular ACSF saturated with 95% O_2/5% CO_2 and maintained at room temperature for at least one hour before electrophysiological recordings.

For electrophysiological experiments, slices were transferred to a recording chamber (Warner Instruments, Hamden, CT, USA) mounted on a fixed upright microscope and continuously perfused (2 to 3 ml/min) with regular ACSF solution saturated with 95% O_2/5% CO_2 and heated to 30 $\pm$ 1°C using a solution heater (Warner Instruments, Hamden, CT, USA). DRN neurons were visualized using Olympus BX51 microscope equipped with a 40X water-immersion objective, differential interference contrast (DIC) and fluorescence systems. Somatic whole-cell recordings from putative DRN 5-HT neurons were performed using patch electrodes with tip resistance of 3 - 5 mΩ, when filled with an internal solution containing (in mM): 120 potassium gluconate; 10 KCl; 10 Na_2-phosphocreatine; 10 HEPES; 1 $MgCl_2$; 1 EGTA; 2 Na_2-ATP; 0.25 Na-GTP (pH 7.3 adjusted with KOH, osmolality 280 - 290 mOsm). In some experiments, TdTomato retrogradely labeled putative DRN 5-HT neurons were visualized using Texas Red fluorescence filter (λ = 540-580 nm) and targeted for whole-cell patch clamp recordings. Membrane current and voltage were amplified with an Axoclamp 2B or Multiclamp 700B amplifier (Molecular Devices, San Jose Union City, CA, USA), filtered at 3 kHz, digitized at 20 kHz with Digidata 1440 and acquired using pClamp 10.7 software (Molecular Devices, San Jose, CA, USA).

Evoked excitatory postsynaptic currents (eEPSCs) were induced by single square-pulses (duration = 100 to 200 μs) delivered at 0.1 Hz and recorded from neurons voltage clamped at -70 mV in the presence of GABAA receptor antagonists picrotoxin (100 μM). To access paired-pulse ratio (PPR), pair of eEPSCs were triggered with an inter-stimulus interval of 50 ms. The intensity of the stimulus was adjusted to evoke 75 % of the maximal amplitude of eEPSCs. The cell-input resistance and access resistance (10 - 20 mΩ) were monitored online throughout the experiments using 10 mV hyperpolarizing voltage steps (500 ms duration). Recordings were discarded when the input and series resistance changed by more than 20 %.

Immunohistochemistry

Rats were deeply anesthetized with pentobarbital and transcardially perfused with 100 ml phosphate buffer saline (PBS) (0.9 %), followed by 250 ml ice-cold 4 % paraformaldehyde (PF) in 1X phosphate buffer (pH 7.4). Brains were removed and post-fixed in 4 % PF for an hour, and immersed in 10 % sucrose solution at 4°C. Coronal sections (40 μm) containing the DRn were cut using a microtome (American Optical 860 model). To block unspecific binding, brain sections containing DRn, were first incubated overnight at 4°C in PB solution containing 10% normal goat serum (NGS) and 0.5 % Triton X-10. The sections were then incubated overnight at 4 °C with the primary antibodies (Mouse anti-Tph2, 1:200 dilution, rabbit anti-RFP, 1:200 dilution, abcam, Waltham, MA, USA) in a PBS solution containing 1 % NGS and 0.5 % Triton X-10. Section were washed in PBS (10 min, 3 times) and incubated with the species-specific secondary antibodies (Goat anti-mouse Alexa 488, Goat anti-rabbit Alexa 594; 1:500, abcam, Waltham, MA, USA) for 5 hours at room temperature. After incubation with secondary antibodies, the sections were washed three time with PBS and mounted on glass slides for fluorescence imaging using Leica DMi8 fluorescence inverted microscope (Leica Microsystems Inc., Buffalo Grove, IL, USA).

QUANTIFICATION AND STATISTICAL ANALYSIS

Glutamate-mediated eEPSCs were analyzed using Clampfit 10.7 software (Molecular Devices, San Jose Union City, CA, USA). The amplitude of eEPSCs was determined by measuring the average current during a 2 ms time window at the peak of each eEPSC and subtracted from baseline current measured during a 5 ms before the stimulus artifact. All eEPSC amplitudes were normalized to the mean baseline amplitude recorded for at least 5 min before administration of OXTR agonists. For paired pulse experiments the paired pulse ratio (PPR = $eEPSC_2/eEPSC_1$) were averaged for at least 60 consecutive trials before and during activation of OXTRs. To determine the coefficient of variation (CV), the standard deviation (SD) and the mean amplitude of eEPSCs were calculated for at least 60 consecutive trials before and during administration of OXTR agonists. The CV was then given by the following ratio (SD) / (eEPSC mean amplitude). Statistical analysis was performed using Origin 8.0 software (OriginLab Co, Northampton, MA, United States). The results in the text and figures are expressed as mean $\pm$ SEM. Parametric paired t-test was used for within group comparison. For comparison between groups, analysis of variance (ANOVA) using post-hoc Bonferroni test was used. Statistical significance was set at $p < 0.05$.